A Method for Series-Resistance-Immune Extraction of Low-Frequency Noise Parameters in Nanoscale MOSFETs

Angeliki Tataridou, Gerard Ghibaudo, Christoforos Theodorou

A Method for Series-Resistance-Immune Extraction of Low Frequency Noise Parameters in Nano-scale MOSFETs

Angeliki Tataridou, *IEEE student member,* Gerard Ghibaudo, *IEEE fellow*, and Christoforos Theodorou

***Abstract*—This paper presents a new methodology for the extraction of low-frequency noise or random telegraph noise parameters, such as the gate oxide interface trap density, N_t, and the mobility fluctuations factor, Ω, without the influence of the source/drain series resistance, R_{sd}. The method utilizes the Y-function -which is immune to any first-order degradation, including the series resistance- as well as the intrinsic mobility degradation factors $\theta_{1,0}$ and θ_2. The proposed extraction technique is first demonstrated through numerical calculations and then applied on experimental results of n-channel short length FinFETs. It is shown that if the R_{sd} impact is not accounted for, the extracted LFN parameters through the classic carrier number fluctuations with correlated mobility fluctuations model (CNF/CMF) can lead to significant extraction errors. This mainly concerns the correlated mobility factor Ω, which may be strongly underestimated, but also the extraction of the trap density N_t.**

***Index Terms*—Low frequency noise, Carrier number fluctuations, Correlated mobility fluctuations, FinFETs, mobility degradation, series-resistance, Remote Coulomb scattering**

I. Introduction

Low-frequency noise (LFN) and Random Telegraph Noise (RTN) effects in MOSFETs [1], [2] have become significant performance limiting factors in advanced nano-scale devices [3] and circuits [4]. The reason is that the amplitude of these trap-related fluctuations is reciprocally proportional to the gate oxide area [2]. Therefore, it is of great importance to properly characterize experimentally these types of noise, and extract the noise model parameters with high accuracy. Apart from helping us gain a better understanding of the fluctuation mechanisms and conclude on interface and material quality, the precise parameter extraction offers a highly valuable input in the development and utilization of noise models in circuit simulations. It is in fact a prerequisite for achieving high accuracy noise-aware circuit design. Traditionally, the main parameters that can be extracted through an LFN experimental characterization in MOSFETs are the volumetric oxide interface trap density, N_t (/cm^3/eV), and the remote Coulomb scattering coefficient, α_{sc} (Vs/C) [5]. Using the carrier number fluctuations (CNF) with correlated mobility fluctuations (CMF) model [5], N_t can be extracted through the flat-band voltage power spectral density $S_{Vfb} = q^2kT\lambda N_t/(WLC_{ox}^2 f)$, where q is the elementary charge, k the Boltzmann constant, T the temperature, C_{ox} the gate oxide capacitance per area, f the frequency and W, L the channel width and length respectively. In recent years, our team has proposed to replace the extraction of the gate voltage sensitive α_{sc} with the extraction of parameter which is bias-independent for a wide range of drain currents, the factor $\Omega = \alpha_{sc}\mu_{eff}C_{ox}$, where μ_{eff} is the effective channel mobility [6]. For long channel devices, this extraction can be sufficiently reliable, however in short channel devices, where the source/drain series resistance (R_{sd}) becomes important with respect to the reduced channel resistance, the extraction process can be jeopardized. The reason behind this issue is the fact that some static parameters which are utilized for noise parameter extraction, such as the transistor gain g_m/I_d, are affected by mobility degradation effects as well as access resistance issues. Concerning the latter, in one of our recent works [7] we demonstrated that the presence of R_{sd} can lead to an underestimation in the extraction of Ω and we suggested to exploit the series resistance immunity of the Y-function ($Y = I_d/\sqrt{g_m}$) [8] in the extraction methodology. Nevertheless, the Y-function is also suppressing the intrinsic first-order mobility attenuation factor $\theta_{1,0}$, which may cause a different type of error in the extracted parameters. In this work we study in detail how both the mobility attenuation and the R_{sd}-related degradation can impact the level of LFN in strong inversion, and explore some modeling approaches to present a new parameter extraction method, independent of these effects. An experimental application of the proposed method on short-channel FinFETs is also presented.

A. Tataridou, G. Ghibaudo, and C. Theodorou are with the Institute of Microelectronics, Electromagnetism and Photonics (IMEP-LAHC), University Grenoble Alpes, University Savoie Mont Blanc, C.N.R.S., Grenoble INP, Grenoble, 38000, France (e-mail: angeliki.tataridou@grenoble-inp.fr, gerard.ghibaudo@grenoble-inp.fr, christoforos.theodorou@grenoble-inp.fr).

II. Impact Of Degradation Effects On LFN

A. Mobility attenuation factors

The channel mobility degradation effects are typically expressed through the conventional model of the effective mobility by introducing the first and second order attenuation factors $\theta_{1,0}$ and θ_2, respectively, through (1) [9]:

$$\mu_{eff} = \frac{\mu_0}{1 + \theta_{1,0}\left(\frac{Q_i}{C_{ox}}\right) + \theta_2\left(\frac{Q_i}{C_{ox}}\right)^2} \quad (1)$$

where μ_{eff} is the effective channel mobility, μ_0 the low-field mobility, Q_i the total inversion charge per unit area.

In order to properly probe the exact impact of these factors on the behavior of LFN, we should begin from the classic carrier number fluctuations with correlated mobility fluctuations (CNF/CMF) approach [5]. According to this generally accepted model, a fluctuation in the oxide charge due to trapping of carriers induces a change in the drain current, ΔI_d, directly through the variation in the number of free carriers and indirectly through a change in the effective mobility due to the trapped charge Q_{ox}. Considering the classical drain current expression in linear region (2), [9], this can be all expressed through (3).

$$I_{d,0} = \frac{W}{L}\mu_{eff}V_d Q_i \tag{2}$$

$$\Delta I_{d,0} = \frac{\partial I_d}{\partial V_g}\frac{\partial V_g}{\partial Q_i}\Delta Q_i + \frac{\partial I_d}{\partial Q_i}\frac{\partial Q_i}{\partial Q_{ox}}\frac{\partial Q_{ox}}{\partial \mu_{eff}}\Delta\mu_{eff} \tag{3}$$

where V_d is the applied drain voltage and V_g the gate voltage.
The index "0" refers to the absence of series resistance, R_{sd}, and μ_{eff} is given by (1). After calculations, we obtain:

$$\left.\frac{\Delta I_d}{I_d}\right|_0 = -\left.\frac{g_m}{I_d}\right|_0 \Delta V_{fb}\left(1 + \Omega\left.\frac{I_d}{g_m}\right|_0\right) \tag{4}$$

where $\Omega = \alpha_{sc}\mu_{eff}C_{ox}$ is the CMF factor [6], $\Delta V_{fb} = Q_{ox}/(WLC_{ox})$ the flat-band voltage fluctuation caused by the trapped charge Q_{ox}, and g_m/I_d the transistor gain calculated as follows:

$$\left.\frac{g_m}{I_d}\right|_0 = \frac{C_{gc}}{Q_i}\left(1 - \frac{Q_i}{C_{gc}}\frac{\theta_{1,0} + 2\theta_2 Q_i/C_{gc}}{1 + \theta_{1,0}\,Q_i/C_{gc} + \theta_2\left(Q_i/C_{gc}\right)^2}\right) \tag{5}$$

where $C_{gc} = dQ_i/dV_g$ is the gate-to-channel capacitance. One can easily notice in (5) that $\theta_{1,0}$ and θ_2 are already accounted for through g_m/I_d in (4). Indeed, as shown in Fig. 1, regardless the presence of mobility degradation or not, the CNF/CMF model captures well the simulated data from weak to strong inversion. The simulation results were obtained in Python using (2), with Q_i numerically calculated using the Lambert-W function [10], and the following parameters: W = 0.1 µm, L = 0.1 µm, µ0 = 100 cm^2/Vs, T = 300 K, η = 1, t_{ox} = 1.2 nm, V_t = 0.2 V and V_d = 30 mV.

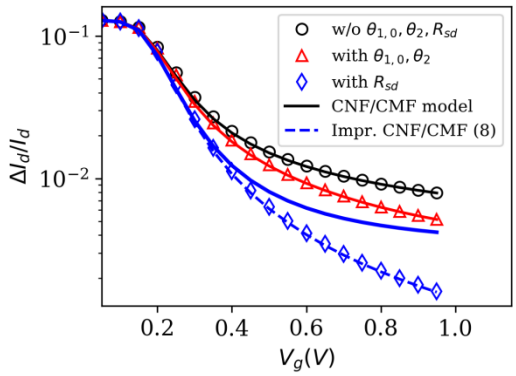

Fig. 1. Simulated data (symbols) and CNF/CMF model (lines) of normalized drain current variation versus gate voltage. Parameters used: $\theta_{1,0}$=1V^{-1}, θ_2=0.5V^{-2}, R_{sd}=1kΩ.

B. Series resistance: a degradation of extrinsic origin

Despite the fact that the effective mobility-related drain current degradation is well accounted for in the CNF/CMF model -as shown in paragraph II.A, this is not necessarily true in the case of an attenuation related to source/drain series resistance, R_{sd}, because it is an extrinsic effect. The simplest way to express this kind of current degradation is through (6):

$$I_d = \frac{I_{d,0}}{1 + G_{d,0}R_{sd}} \tag{6}$$

where $G_{d,0} = dI_{d,0}/dV_d$ is the intrinsic channel conductance. It can be easily proven that the total derivative of (6) is:

$$dI_d = \frac{dI_{d,0}}{\left(1 + G_{d,0}R_{sd}\right)^2} \overset{(6)}{\Leftrightarrow} \frac{\Delta I_d}{I_d} = \left.\frac{\Delta I_d}{I_d}\right|_0 \frac{1}{\left(1 + G_{d,0}R_{sd}\right)} \tag{7}$$

Combining (7) with (4) results in (8):

$$\frac{\Delta I_d}{I_d} = -\frac{g_m}{I_d}\Delta V_{fb}\left(1 + \Omega\left.\frac{I_d}{g_m}\right|_0\right) \tag{8}$$

Note how the CNF part ($g_m/I_d\Delta V_{fb}$) includes the impact of R_{sd}, whereas the parenthesis expressing the impact of CMF is not affected by R_{sd}. As a result, if we use the measured I_d/g_m instead of the intrinsic $I_d/g_m|_0$ (without R_{sd}), the model is not expected to fit the measured data. This effect is shown in Fig. 1, where it is evident that although $\theta_{1,0}$ and θ_2 are not affecting the model's accuracy, R_{sd} can cause a significant deviation from the simulated data, mainly in strong inversion. In fact, there is a perfect fit when we use the improved CNF/CMF as proposed through (8).

It is also interesting to examine how this effect can impact the extraction accuracy of the CMF factor Ω. Ω is usually extracted using the input-referred gate voltage noise $\Delta V_g = \Delta I_d/g_m$ (or $\sqrt{S_{Vg}} = \sqrt{S_{Id}}/g_m$ for PSD analysis) [5], to take advantage of its linear dependence with I_d/g_m and extract Ω using the slope:

$$\Delta V_g = -\Delta V_{fb}\left(1 + \Omega\left.\frac{I_d}{g_m}\right|_0\right) \tag{9}$$

This quantity is plotted in Fig. 2, versus both gate voltage overdrive V_g-V_t and I_d/g_m. As expected, the CNF/CMF model using the measured I_d/g_m cannot predict the noise behavior when R_{sd} is non-negligible. Furthermore, comparing these two figures leads us to conclude that while ΔV_g does not seem affected by R_{sd}, when plotted against I_d/g_m, it seems as if it was degraded. This can be attributed to the increase of I_d/g_m with R_{sd}, which in turn leads to a less steep slope and to an eventual underestimation in the extraction of Ω, as shown in [7]. It is also obvious that it might result in an overestimation of ΔV_{fb}.

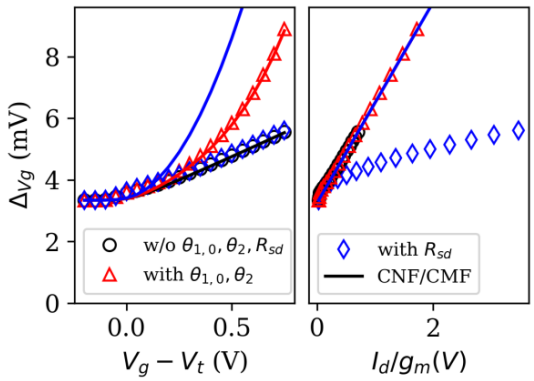

Fig. 2. Simulated data (symbols) and CNF/CMF model (lines) of input-referred gate voltage variation versus gate voltage overdrive (left) and I_d/g_m (right). Parameters used: $\theta_{1,0}$=1V^{-1}, θ_2=0.5V^{-2}, R_{sd}=1kΩ.

III. Proposed Methodology For Suppressing The Impact Of Rsd

As was demonstrated in part II, in order to achieve an accurate extraction of LFN parameters when R_{sd} is important, we need a precise estimation of $I_d/g_m|_0$. A quantity that is completely immune to R_{sd} is the Y-function, which is defined through $Y = I_d/\sqrt{g_m}$. As shown in [7], in the ideal case when θ_1=θ_2=0, $I_d/g_m|_0$ can be very well approximated with $Y/\sqrt{(\beta V_d)}$, where $\beta = W\mu_0 C_{ox}/L$. However, as

demonstrated in [11], a more accurate approach of $I_d/g_m|_0$ is needed to

$$\left.\frac{I_d}{g_m}\right|_0 = \frac{\eta kT}{q} + \frac{Y}{\sqrt{\beta V_d}}\left(1 + \theta_{1,0}\frac{Y}{\sqrt{\beta V_d}} + \theta_2\left(\frac{Y}{\sqrt{\beta V_d}}\right)^2\right) \quad (10)$$

Equation (10) is actually a simplification of (5), which, if inverted, gives:

$$\left.\frac{I_d}{g_m}\right|_0 = \frac{Q_i}{C_{gc}}\left(\frac{1 + \theta_{1,0}\,Q_i/C_{gc} + \theta_2\left(Q_i/C_{gc}\right)^2}{1 - \theta_2\left(Q_i/C_{gc}\right)^2}\right) \quad (11)$$

and Q_i/C_{gc} is well approximated with $Y\sqrt{(\beta V_d)}$. However, in the presence of θ_2, the Y-function in strong inversion should be corrected as shown in [12]. Thus, for $V_g > V_t$, (11) can be evaluated using the corrected Y-function, Y_n, as:

$$\left.\frac{I_d}{g_m}\right|_0 = \frac{\eta kT}{q} + Y_n\left(\frac{1 + \theta_{1,0}Y_n + \theta_2(Y_n)^2}{1 - \theta_2(Y_n)^2}\right) \quad (12a)$$

$$Y_n = Y\sqrt{\frac{\left(1 - \theta_2\left(V_g - V_t\right)^2\right)}{\beta V_d}} \quad (12b)$$

Fig. 3 illustrates how (12) can perfectly emulate $I_d/g_m|_0$, and how it can ensure a proper extraction of S_{Vfb} and Ω through linear regression.

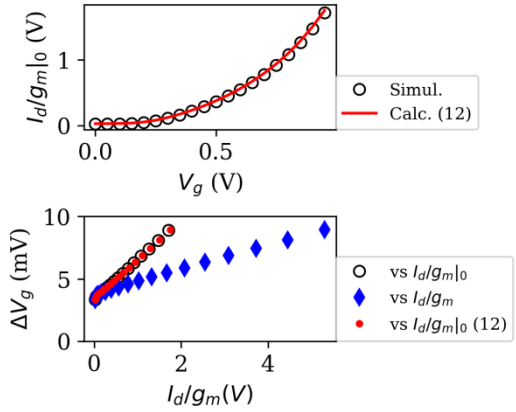

Fig. 3. Comparison between simulated $I_d/g_m|_0$ and calculated through (12) (top). Simulated data of input-referred gate voltage variation versus I_d/g_m, simulated with and without the R_{sd} impact and calculated through (12) (bottom). Parameters used: R_{sd}=1kΩ.

IV. Experimental Application Of The Method

The method presented above requires the extraction of several device parameters from static measurements: V_t, β, $\theta_{1,0}$ and θ_2. Then the $I_d/g_m|_0$ can be calculated using (12) and applied on the CNF/CMF model (15). We applied the proposed methodology on n-channel FinFETs fabricated at IMEC-Leuven with number of fins 4, fin height H_{fin} = 26 nm, and fin width W_{fin} =6 nm. In order to extract the $\theta_{1,0}$ coefficient we performed I_d-V_g measurements for 3 different channel lengths, L= 44,70 and 90 nm, in the linear region (V_d = 30 mV), using the programmable bias point probe system NOISYS7 by Synergie Concept [13], combined with a semi-auto 300 mm Cascade Micro Tech probe station . After extracting the V_t and β parameters using the Y-function method, we extracted the effective mobility attenuation coefficients θ_1 and θ_2 from the linear fit of the θ_{eff} quantity, as given by (13), versus V_g -V_t in the strong inversion region [12]. A representative example of the θ_1 and θ_2 extraction is shown in fig.4. The extracted values of θ_2 were between 0.1 and 0.3 V^{-2} in all cases.

account for $\theta_{1,0}$ and θ_2.

$$\Theta_{eff}(V_g) = \frac{\beta V_d}{I_d} - \frac{1}{V_g - V_t} = \theta_1 + \theta_2(V_g - V_t) \quad (13)$$

The dependence of θ_1 on R_{sd}, as given by (14), allows the extraction of $\theta_{1,0}$ and R_{sd} when θ_1 is plotted with β for different channel lengths as shown in Fig. 4. It should be noted that the static parameters θ_1, θ_2, β and V_t, were extracted by the average I-V characteristic of 9 devices for the case of channel length 70 and 90 nm and of 41 devices for the 44 nm channel length.

$$\theta_1 = \theta_{1,0} + \beta R_{sd} \quad (14)$$

$\theta_{1,0}$ and R_{sd}, normalized by the effective gate oxide width, were extracted to be 0.497 V^{-1} and 203 Ω·μm respectively.

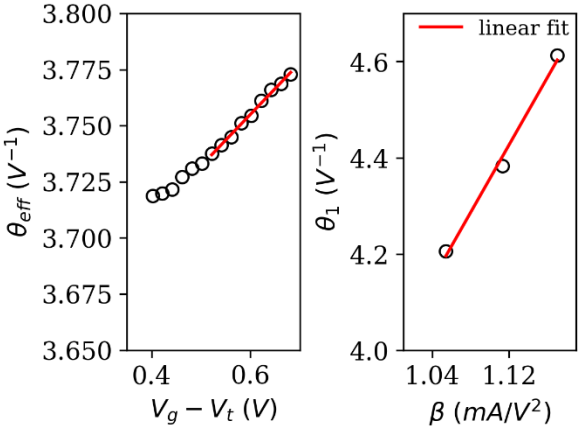

Fig. 4. Θ_{eff} vs (V_g-V_t) for channel length 90 nm along with the linear fit (left). First order mobility attenuation factor (θ_1) vs β for 3 different channel lengths (44, 70, and 90 nm) along with the linear fit (right).

In order to avoid the variability effect in our LFN analysis, we measured 41 devices for L = 44 nm, and we extracted an average I_d-V_g curve, from which we calculated g_m and the Y-function. The curves and the extracted subthreshold slope SS, which we need in order to calculate the ideality factor η = qSS / (kTln(10)) [14], used in (12), are shown in Fig.5. The ideality factor was extracted to be η = 1.13.

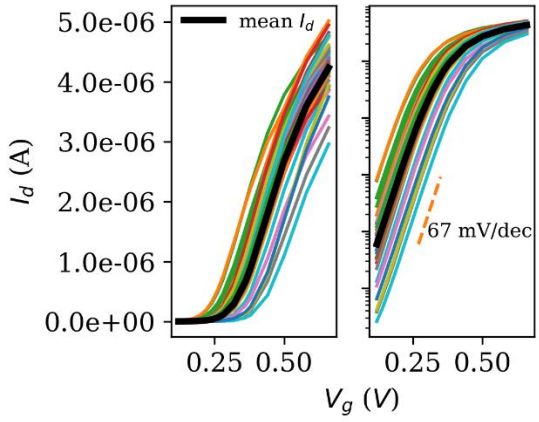

Fig. 5. Current-Voltage characteristics in linear and logarithmic scale of 41 dies along with the average Id-Vg curve, extracted by taking the mean value of the drain current of each device.

Detailed LFN measurements were also performed and the input-referred gate voltage noise power spectral density $S_{Vg}=S_{id}/g_m^2$ was extracted for 41 devices at various gate voltage values. The spectra, along with the average spectrum, extracted by taking the mean logarithmic [15] value of S_{Vg} of each device, are shown in Fig. 6. The 1/f behavior of the average spectrum allows the application of

the CNF/CMF model as it can be considered that a uniform trap distribution is present for each bias condition.

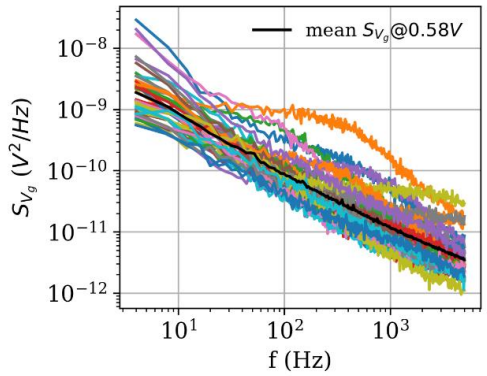

Fig. 6. Input-referred gate voltage noise vs frequency, for 41 devices with L = 44 nm, biased under V_g= 0.58 V.

Fig. 7 shows the $\sqrt{S_{Vg}}$ extracted at 10 Hz vs both the measured I_d/g_m and the calculated $I_d/g_m|_0$ using (12), for the extraction of the flat-band voltage power spectral density, S_{Vfb} and the Ω component, using the generalized form of (9) for the linear fit in strong inversion.

$$\sqrt{S_{Vg}} = \sqrt{S_{Vfb}}\left(1 + \Omega \left.\frac{I_d}{g_m}\right|_0\right) \qquad (15)$$

It should be noted that S_{Vfb} is actually the equivalent of Δ_{Vfb} when going from a single trap to a distribution of traps. Δ_{Vfb} refers to the electrostatic impact of a trapped charge Q_{ox} whereas S_{Vfb} is the flat-band voltage power spectral density caused by a fluctuating oxide charge, S_{Qox}. Therefore, Δ_{Vg} is more useful when simulating the noise amplitude behavior or studying single trapping effects such as RTN, but S_{Vg} is necessary for studying 1/f noise, where a distribution of trap time constants is involved.

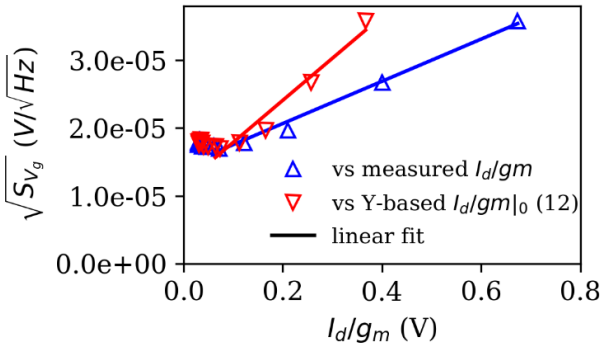

Fig. 7. Square root of input-referred noise, $\sqrt{S_{Vg}}$, versus the measured ratio of drain current and transconductance, I_d/g_m, and the calculated one using (12) along with the strong inversion linear fit based on (9).

Table I shows the extracted values of $N_t = S_{Vfb}WLC_{ox}^2f / \lambda q^2kT$ and Ω with both the measured I_d/g_m and the R_{sd}-free $I_d/g_m|_0$ (12). As it can be seen, there is a slight overestimation of N_t with the classical method. More importantly, the Ω component seems to be highly influenced by the I_d/g_m values used, as explained in part II. In fact, the new Ω is more than two times higher, revealing a much more critical magnitude of the remote Coulomb scattering.

TABLE I
N_T AND Ω EXTRACTED VALUES

	Measured I_d/g_m	$I_d/g_m|_0$ as calculated by (12)
N_T (eV/cm^3)	$5.13\text{x}10^{16}$	$3.36\text{x}10^{16}$
Ω (V^{-1})	2.15	5.29

V. Conclusion

A complete, R_{sd}-immune methodology has been proposed for the accurate extraction of CNF/CMF noise model parameters, such as N_t and Ω. An I_d/g_m independent of R_{sd} is extracted using the the Y-function properties, thus any questionable issues on the accuracy of the LFN extracted parameters due to the R_{sd} presence have been overcome. This method was successfully applied in experimental measurements performed on short-channel n-FinFETs. It was revealed that the extraction of Ω using the classical method, with no suppression of the series resistance impact, was underestimated by more than a factor of two.

Acknowledgment

The authors would like to acknowledge the Horizon 2020 ASCENT EU project (Access to European Nanoelectronics Network -Project no. 654384). They would also like to thank Thomas Chiarella and Jerome Mitard from IMEC-Leuven for their technical help and general support.

References

[1] G. Reimbold, "Modified 1/f Trapping Noise Theory and Experiments in MOS Transistors Biased from Weak to Strong Inversion—Influence of Interface States," *IEEE Trans. Electron Devices*, vol. 31, no. 9, pp. 1190–1198, 1984,DOI:10.1109/T-ED.1984.21687.

[2] K. K. Hung, P. K. Ko, C. Hu, and Y. C. Cheng, "Random telegraph noise of deep-submicrometer MOSFETs," *IEEE Electron Device Lett.*, vol. 11, no. 2, pp. 90–92, 1990,DOI:10.1109/55.46938.

[3] B. Kaczer *et al.*, "The defect-centric perspective of device and circuit reliability - From individual defects to circuits," *Eur. Solid-State Device Res. Conf.*, vol. 2015-Novem, pp. 218–225, 2015,DOI:10.1109/ESSDERC.2015.7324754.

[4] K. Takeuchi *et al.*, "Direct observation of RTN-induced SRAM failure by accelerated testing and its application to product reliability assessment," *Dig. Tech. Pap. - Symp. VLSI Technol.*, pp. 189–190, 2010,DOI:10.1109/VLSIT.2010.5556222.

[5] G. Ghibaudo, O. Roux, C. Nguyen-Duc, F. Balestra, and J. Brini, "Improved Analysis of Low Frequency Noise in Field-Effect MOS Transistors," *Phys. Status Solidi*, vol. 124, no. 2, pp. 571–581, 1991,DOI:10.1002/pssa.2211240225.

[6] E. G. Ioannidis, C. A. Dimitriadis, S. Haendler, R. A. Bianchi, J. Jomaah, and G. Ghibaudo, "Improved analysis and modeling of low-frequency noise in nanoscale MOSFETs," *Solid. State. Electron.*, vol. 76, pp. 54–59, 2012,DOI:10.1016/j.sse.2012.05.035.

[7] A. Tataridou, G. Ghibaudo, and C. Theodorou, "Influence of series resistance on the experimental extraction of FinFET noise parameters," in *International Conference on Microelectronic Test Structures*, 2020.

[8] G. Ghibaudo, "New method for the extraction of MOSFET parameters," *Electron. Lett.*, 1988,DOI:10.1049/el:19880369.

[9] G. Ghibaudo, "Analytical modelling of the MOS transistor," *Phys. status solidi*, 1989,DOI:10.1002/pssa.2211130127.

[10] T. A. Karatsori *et al.*, "Full gate voltage range Lambert-function based methodology for FDSOI MOSFET parameter extraction," *Solid. State. Electron.*, vol. 111, 2015,DOI:10.1016/j.sse.2015.06.002.

[11] J. B. Henry, A. Cros, J. Rosa, Q. Rafhay, and G. Ghibaudo, "Impact of access resistance on New-Y function methodology for MOSFET parameter extraction in advanced FD-SOI technology," *IEEE Int. Conf. Microelectron. Test Struct.*, vol. 0, pp. 0–4, 2017,DOI:10.1109/ICMTS.2017.7954269.

[12] C. Mourrain, B. Cretu, G. Ghibaudo, and P. Cottin, "New method for parameter extraction in deep submicrometer MOSFETs," in *IEEE International Conference on Microelectronic Test Structures*, 2000.

[13] J. A. Chroboczek, A. Szewczyk, and G. Piantino, "Low frequency noise point probe measurements on a wafer level using a novel programmable current amplifier," in *Noise in Physical Systems and 1/F Fluctuations*, 2001, pp. 701–704.

[14] J. P. Colinge, R. W. Bower, and G. Editors, "Silicon-on-Insulator Technology," *MRS Bull.*, 1998,DOI:10.1557/S0883769400029766.

[15] C. G. Theodorou *et al.*, "Low frequency noise variability in ultra scaled FD-SOI n-MOSFETs: Dependence on gate bias, frequency and temperature,"*Solid.State.Electron.*,vol.117,pp.88–93,2016, DOI:10.1016/j.sse.2015.11.011